Reconstitution of [Fe]-hydrogenase using model complexes

Seigo Shima[1,2,*], Dafa Chen[3], Tao Xu[4], Matthew D. Wodrich[4,5], Takashi Fujishiro[1], Katherine M. Schultz[4], Jörg Kahnt[1], Kenichi Ataka[6] & Xile Hu[4,*]

[1]Max Planck Institute for Terrestrial Microbiology, 35043 Marburg, Germany.

[2]PRESTO, Japan Science and Technology Agency (JST), 332-0012 Saitama, Japan.

[3]School of Chemical Engineering and Technology, Harbin Institute of Technology, 150001 Harbin, China.

[4]Laboratory of Inorganic Synthesis and Catalysis, Institute of Chemical Science and Engineering, Ecole Polytechnique Fédérale de Lausanne (EPFL), 1015 Lausanne, Switzerland.

[5]Laboratory for Computational Molecular Design, Institute of Chemical Science and Engineering, Ecole Polytechnique Fédérale de Lausanne (EPFL), 1015 Lausanne, Switzerland.

[6]Department of Physics, Freie Universität Berlin, 14195 Berlin, Germany.

Abstract. [Fe]-Hydrogenase catalyzes the reversible hydrogenation of a methenyl-tetrahydromethanopterin substrate, which is an intermediate step during methanogenesis from CO_2 and H_2. The active site contains an iron-guanylylpyridinol (FeGP) cofactor, in which Fe^{2+} is coordinated by two CO ligands, as well as an acyl carbon atom and a pyridinyl nitrogen atom from a 3,4,5,6-substituted 2-pyridinol ligand. However, the mechanism of H_2 activation by [Fe]-hydrogenase is unclear. Here, we report reconstitution of [Fe]-hydrogenase from an apoenzyme using two FeGP cofactor mimics to create semi-synthetic enzymes. The small molecule mimics reproduce the ligand environment of the active site, but are inactive towards H_2 binding and activation on their own. We show that reconstituting the enzyme using a mimic containing a 2-hydroxy pyridine group restores activity, whilst an analogous experiment with a 2-methoxy-pyridine complex was essentially inactive. These findings, together with DFT computations, support a mechanism in which the 2-hydroxy group is deprotonated before serving as an internal base for heterolytic H_2 cleavage.

Table of content summary

[Fe]-Hydrogenase has an iron-guanylylpyridinol cofactor and catalyzes the reversible hydrogenation of a methenyl-tetrahydromethanopterin. We reconstituted [Fe]-hydrogenase using cofactor mimics. The enzyme containing the mimic with a 2-hydroxy-pyridine group was active, while that containing a 2-methoxy-pyridine group was inactive. This result, together with DFT computations, supports a catalytic mechanism involving the deprotonated pyridinol hydroxy group as proton acceptor.

Table of content graph

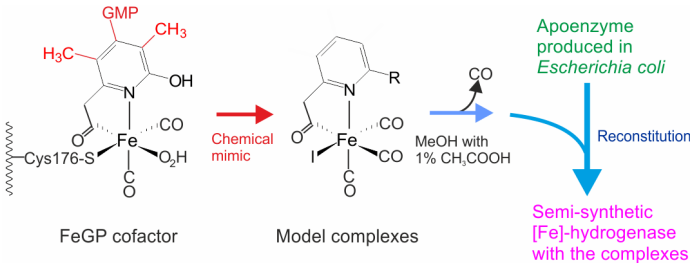

(90 mm x 40 mm)

Future H_2-utilizing technologies rely upon the development of new catalysts for activating H_2. Robust, efficient, and inexpensive catalysts must be developed, for which nature provides intriguing design principles. In the microbial world, H_2 is produced and utilized in energy metabolism, with the corresponding reactions being catalyzed by hydrogenases[1]. The three known types of hydrogenases commonly catalyze reversible cleavage of H_2 to a proton and a hydride ion as an initial step. Two of the hydrogenases contain a dinuclear metal centre, either [NiFe] or [FeFe], and further catalyze the extraction of two electrons from the hydride[2,3]. The third hydrogenase, [Fe]-hydrogenase (Hmd), transfers the hydride ion to the methenyl-tetrahydromethanopterin (methenyl-H_4MPT^+) substrate, which is an intermediate in the formation of methane from H_2 and CO_2 mediated by hydrogenotrophic methanogenic archaea (Fig. 1a)[4,5].

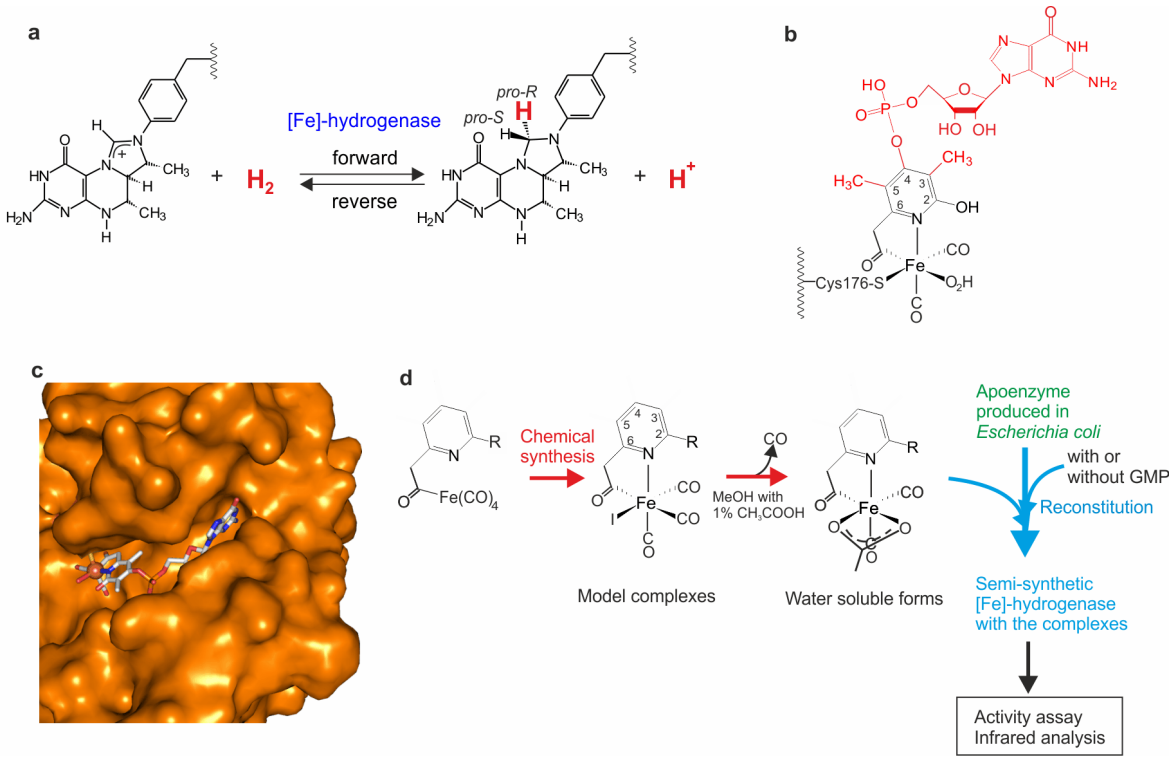

Figure 1 | Reaction catalyzed by [Fe]-hydrogenase and reconstitution of [Fe]-hydrogenase with the model complexes of the iron-guanylylpyridinol (FeGP) cofactor. a, Reaction catalyzed by [Fe]-hydrogenase. **b,** Chemical structure of the FeGP cofactor. The groups lacking in the model complexes used in this work are highlighted in red. **c**, Stick

model (with protein surface model) of the FeGP cofactor covalently bound via cysteine 176 to [Fe]-hydrogenase. Carbon, nitrogen, oxygen, phosphorous and sulphur atoms are depicted in gray, blue, red, orange, and yellow, respectively. The iron atom is shown as brown sphere. **d**, An overview of the strategy for reconstituting semi-synthetic [Fe]-hydrogenase from apoenzyme biologically produced in recombinant *Escherichia coli* and the chemically synthesized model complexes.

[Fe]-Hydrogenase contains a single iron in the iron-guanylylpyridinol (FeGP) cofactor at the active site (Fig. 1b and c). This cofactor can be isolated from the denatured native [Fe]-hydrogenase holoenzyme (protein with cofactor)[6,7]. Fully active [Fe]-hydrogenase can be reconstituted by mixing the [Fe]-hydrogenase apoenzyme (protein without cofactor) and the isolated FeGP cofactor[4,6,8]. The iron centre of the FeGP cofactor is coordinated to two *cis*-CO ligands, the acyl carbon and pyridinyl nitrogen atoms of a pyridinol ligand, and a cysteine sulphur atom (Fig. 1b). The Guanosine monophosphate (GMP) moiety of the FeGP cofactor significantly contributes to binding of the cofactor to the enzyme (Fig. 1c)[4,7,8]. Whereas the structure and properties of [Fe]-hydrogenase have been thoroughly studied, the mechanism of H_2 activation remains speculative. A working hypothesis requires explanation of the following observations: (1) The extracted FeGP cofactor is inactive for H_2 binding; (2) H_2 can interact with the iron centre in the holoenzyme only after the binding of methenyl-H_4MPT^+ to the enzyme, which converts the enzyme from an open to a closed conformation[9,10].

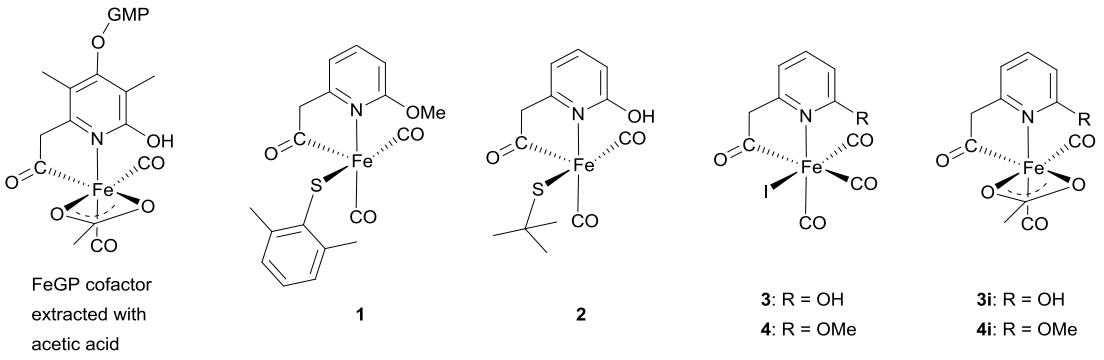

Figure 2 | Structures of synthetic models of [Fe]-hydrogenase. Complexes **1** and **2** both reproduce the first coordination sphere of the active site, but contain a methoxy and a hydroxy group at the second coordination sphere, respectively. Our strategy for reconstitution of semi-synthetic [Fe]-hydrogenase is to substitute a labile ligand of a mimic with cysteine176 of the apoenzyme. Due to their higher stability and solubility, complexes **3** and **4** instead of **1** and **2** were used for reconstitution. To dissolve **3** and **4** in aqueous solutions, these compounds were first dissolved in 99% methanol containing 1% acetic acid, in which they were probably converted to **3i** and **4i**, respectively.

A number of complexes modelling the active site of [Fe]-hydrogenase have previously been synthesized [11-17]. Recently, we prepared complexes **1** and **2**, which reproduce the key features of the active site including the complete donor set, the unusual acylmethylpyridinyl ligation, and in the case of **2**, the hydroxy group at the second coordination sphere (Fig. 2).[12,13] According to the infrared (IR) spectra, both model complexes have *cis*-CO ligands and similar electronic properties to the FeGP cofactor bound in [Fe]-hydrogenase. However, they neither bind nor activate H_2, which is distinct from mimics of [NiFe]- and [FeFe]-hydrogenases, some of which can heterolytically split H_2 and catalyze H_2 oxidation reactions.[18-21] In the case of the isolated FeGP cofactor, its open-coordination site is blocked by 2-mercaptoethanol or acetate,[8,22] which might inhibit the endogenous catalytic activity of

this cofactor. However, the inactivity of complexes **1** and **2** is not due to coordinative saturation, because one of the Fe-coordination sites is unoccupied.

The origin of the inactivity of **1** and **2** was probed by DFT computations. Several DFT studies[23-25] suggest that [Fe]-hydrogenase coordinates and splits H_2 heterolytically using the cysteine thiolate ligand as a proton acceptor to form a Fe hydride intermediate. A similar mechanism was used for computing model complexes (ref. 26-27 and Supplementary Fig. 1). It was found that binding of H_2 is about 43 and 49 kJ/mol uphill for complexes **1** and **2**, respectively, while the splitting of H_2 has a further barrier of 66 and 53 kJ/mol.[26,27] The overall barrier of more than 100 kJ/mol is consistent with the inactivity of **1** and **2** towards H_2 activation. On the other hand, the enzymatic reaction has a barrier of about 50 kJ/mol.[28,29] Given that the FeGP cofactor is only active when bound in the enzyme, we hypothesized that the inactivity of model complexes **1** and **2** arises from the lack of a protein environment. If these complexes could be placed in the same protein environment as the FeGP cofactor, they might become catalytically active. This reasoning was inspired by the recent reports of the reconstitution of highly active [FeFe]-hydrogenase from apoenzyme and less active synthetic models.[30-32] Here, we report the successful incorporation of model complexes into the [Fe]-hydrogenase apoenzyme, which leads to new insights into the mechanism.

Results.

Reconstitution using complex 3. In [Fe]-hydrogenase, the active site is covalently bound to the protein only through the cysteine 176 group. Our strategy for reconstitution is to substitute a labile ligand of a mimic with cysteine176 of the apoenzyme. Analogous ligand substitution chemistry was previously reported for the model complexes.[12,13] Complexes **1** and **2** were prepared in this manner from precursors **4** and **3**, respectively (Fig. 2). As **2** is the most faithful mimic, we started the reconstitution using complex **3**. Water-insoluble **3** was dissolved in 99% methanol containing 1% acetic acid (methanol/acetic acid), in which **3** was

probably converted to intermediate **3i,** as revealed by the IR spectrum after solvent evaporation (Fig.3). This IR spectrum resembled that of the FeGP cofactor extracted with acetic acid (Fig. 3)[22], which shows the presence of only two CO ligands, indicating that dissolution in methanol/acetic acid leads to the loss of one CO ligand in **3**. Both CO stretching frequencies of **3i** were slightly higher than those of the FeGP cofactor extracted with acetic acid, which is consistent with the lack of electron-donating GMP and methyl groups in **3i**. The IR spectrum of **3i** is very similar to that of the isolated iron acetate complex formed upon the reaction of **3** with silver acetate [13]. To reconstitute the holoenzyme, an excess amount of dissolved **3i** was mixed with the [Fe]-hydrogenase apoenzyme from *Methanocaldococcus jannaschii* heterologously produced in *Escherichia coli* (Methods).

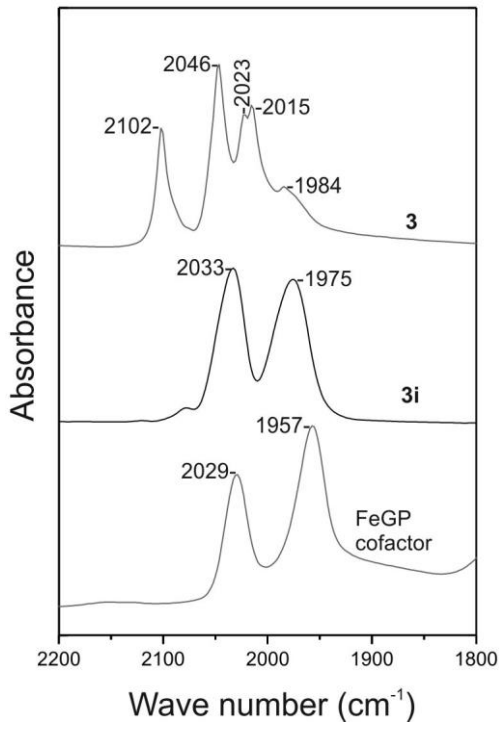

Figure 3 | IR spectra of the model complexes and FeGP cofactor. Powder of **3** with potassium bromide (top), **3i** dissolved in 1% acetic acid in methanol (middle), and the FeGP

cofactor extracted with acetic acid (bottom; spectrum from ref. 22). The spectra indicate that dissolution in methanol/acetic acid leads to the loss of one CO ligand in **3**.

The activity of [Fe]-hydrogenase reconstituted with **3i** at 40 °C was photometrically measured for both the forward (reduction of methenyl-H_4MPT^+ with H_2) and the reverse reactions (H_2 production from methylene-H_4MPT) (reaction scheme shown in Fig. 1a)(Methods)[33]. The absorbance at 336 nm of methenyl-H_4MPT^+ decreased and increased in the forward and reverse reactions, respectively (Fig. 4a and b). With the apoenzyme or **3i** (dissolved in methanol/acetic acid) alone, the spectra of methenyl-H_4MPT^+ and methylene-H_4MPT were unchanged (Fig. 4c and d). The production of H_2 from methylene-H_4MPT in the reverse reaction was detected by gas chromatography (Fig. 4e); the specific activity of H_2 formation was in agreement with that determined in the photometric assay. The specific activities of the reconstituted enzyme in the forward and reverse reactions under standard assay conditions were 3 U/mg and 2 U/mg, respectively. The corresponding turnover frequencies are 2 s^{-1} and 1 s^{-1}, respectively. These rates are very high compared to synthetic hydrogenation catalysts[34,35], which have turnover frequencies typically between 10^{-3} to 0.1 s^{-1}, and only in exceptional cases, have turnover frequencies on the order of 1 s^{-1}. The specific activities of the reconstituted enzymes are approximately 1% of those of the native enzyme. From the Arrhenius equation, a 100-fold decrease in the reaction rate corresponds to an increase of only ~12 kJ/mol in the activation energy, whereas the activation energy of the [Fe]-hydrogenase catalyzed reaction is ~50 kJ/mol[28,29].

The apparent K_m values for methenyl- and methylene-H_4MPT are similar to that of the native enzyme (Supplementary Fig. 2)[29]. The apparent K_m for H_2 was substantially higher than that of the native enzyme (Supplementary Fig. 3). The optimal pH for the H_2-producing activity was lower than that of the native enzyme (Supplementary Fig. 4). The reconstituted enzyme was inhibited by *p*-toluenesulfonylmethyl isocyanide, a strong specific inhibitor of [Fe]-

hydrogenase[36], but the inhibition constant (K_i = 30 nM) was higher than that of the native enzyme (K_i = 1 nM). The enzyme reconstituted in the presence of 2 mM GMP exhibited approximately a two-fold higher specific activity than in the absence of GMP (Supplementary Fig. 5a). The addition of GMP after incorporation of **3i** also increased the activity roughly two-fold. The addition of other nucleoside monophosphates (i.e. AMP, CMP and UMP) into the reconstitution solutions did not affect the activity of the reconstituted enzyme. Maximal reconstitution of the active holoenzyme took 1 h (Supplementary Fig. 6). Kinetic profiles of the complex incorporation were similar in the absence and presence of GMP.

The stoichiometry of the complexes was determined using peak area ratios of the CO and protein-amide II bands in the IR spectra of the reconstituted enzymes (Supplementary Table 1). These data indicated that the occupancy of **3i** in the reconstituted enzymes with GMP was approximately 50%. Based on the stoichiometric data, the specific activity of the reconstituted [Fe]-hydrogenase should be two times higher than described above.

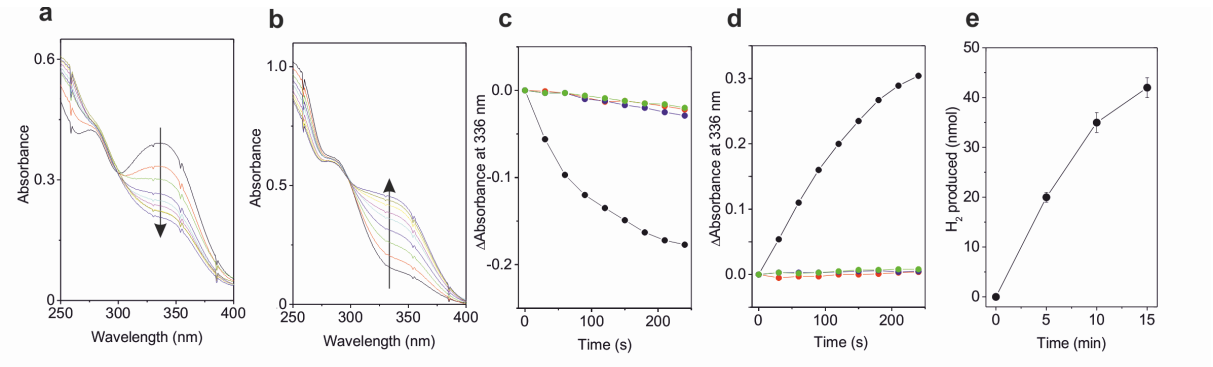

Figure 4 | Activity of the [Fe]-hydrogenase holoenzyme reconstituted with model compound 3i. a, Consumption and **b**, formation of methenyl-H_4MPT^+ were detected (direction of the reactions is indicated by arrows); the changes of absorbance at 336 nm of the consumption and formation reactions were plotted in **c** and **d**, respectively. In the absence of **3i** (blue), the apoenzyme (red), and both **3i** and the apoenzyme (green) in the reconstitution mixture, no activity was detected (**c** and **d**) (Methods). The spectral changes were measured at

least three times. **e**, Production of H_2 in the assay (Methods). Error bars determined by the standard deviation of three measurements**.**

The IR spectrum of the reconstituted [Fe]-hydrogenase with **3i** in the absence of GMP (Fig. 5a) (Methods) shows that the peak positions of the dominant bands at ~ 2020 cm^{-1} and 1945 cm^{-1} are similar to those of the [Fe]-hydrogenase holoenzyme reconstituted with the FeGP cofactor (2011 cm^{-1} and 1944 cm^{-1})[8,36,37]. This suggests incorporation of **3i** into the active site. The IR spectrum also exhibits a number of minor peaks, indicative of a certain amount of **3i** that was unspecifically bound (Supplementary Table 1). When the [Fe]-hydrogenase was reconstituted in the presence of 2 mM GMP, the number of minor peaks in the IR spectrum recorded in the absence of GMP were significantly reduced, and the spectrum exhibited two major peaks at 2016 and 1944 cm^{-1}. This spectrum resembles that of native [Fe]-hydrogenase, although minor peaks at 2073 and 2035 cm^{-1} remained in the former (Fig. 5a). Thus, the presence of GMP apparently leads to improved binding of model complex with the apoenzyme.

In the native holoenzyme the iron is coordinated by cysteine 176. A C176A mutant apoenzyme was then used for reconstitution with **3i**. The IR spectrum in the absence of GMP exhibits many peaks in the region where CO vibrations occur (Fig. 5b). Adding GMP did not significantly reduce the number of CO bands, or convert the spectrum into two major peaks (Fig. 5b), as was the case for reconstitution using the native holoenzyme. In all cases, the ratio of **3i** to protein was around two-fold (Supplementary Table 1). These data suggest that **3i** was either unspecifically bound to the C176A mutant apoenzyme, or was bound in the active site but with a different coordination environment than that of the native enzyme due to the absence of the Cys176 thiolate ligand. The reconstituted C176A enzymes with **3i** in the presence and absence of GMP showed no enzyme activity. This result is consistent with the previous finding that the C176A enzyme reconstituted with the FeGP cofactor is inactive.[38] In

the latter case, the FeGP cofactor is coordinated to an exogenous dithiothreitol ligand, which is required to stabilize the cofactor. In the current case, the iron centre is probably coordinated to an acetate ligand present in the reaction medium. Thus, cysteine 176 is important for the correct binding of the FeGP cofactor or **3i** in the active site, which is required for activity.

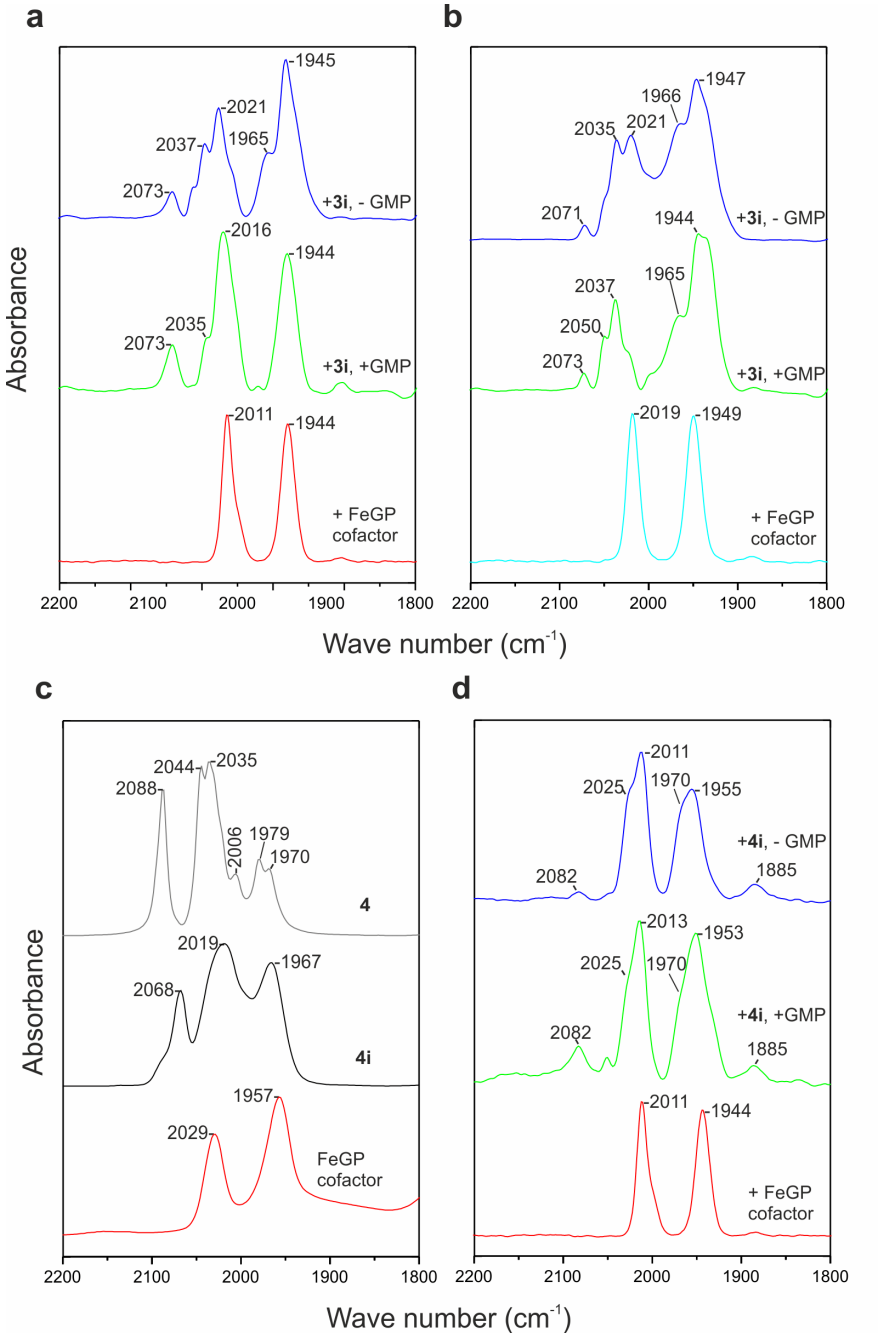

Figure 5 | IR spectra of the [Fe]-hydrogenases reconstituted with 3i and 4i. a, Wild-type [Fe]-hydrogenase reconstituted with **3i** in the absence (top) and presence (middle) of 2 mM GMP, and [Fe]-hydrogenase reconstituted with the FeGP cofactor (bottom). **b**, C176A [Fe]-

hydrogenase reconstituted with **3i** in the absence (top) and presence (middle) of 2 mM GMP, and the C176A [Fe]-hydrogenase reconstituted with the FeGP cofactor (bottom). **c**, Powder of **4** with potassium bromide (top), **4i** dissolved in 1% acetic acid in methanol (middle), and the FeGP cofactor extracted with acetic acid (bottom; spectrum from ref. 22). **d**, Wild-type [Fe]-hydrogenase reconstituted with **4i** in the absence (top) and presence (middle) of 2 mM GMP, and wild-type [Fe]-hydrogenase reconstituted with the FeGP cofactor (bottom). The IR spectra suggest successful incorporation of **3i** and **4i** in the apoenzyme of [Fe]-hydrogenase. The spectra also suggest that the presence of GMP leads to improved binding of **3i** to the apoenzyme, and cysteine 176 is important for the correct binding.

Reconstitution using complex 4. Recent studies suggest that the 2-hydroxy group of the pyridinol ring of the FeGP cofactor might be important for H_2 activation[39,40]. To directly test the importance of the hydroxy group, we used compound **4**, which has a 2-methoxy group at the pyridine ring for the reconstitution of [Fe]-hydrogenase (Fig. 2). When dissolved in methanol/acetic acid, compound **4** was partially converted to **4i,** revealed by an IR spectrum with two broad CO bands at 2019 and 1967 cm^{-1} (Fig. 5c).

Likely owing to the high hydrophobicity of **4i**, an excess amount of this complex unspecifically binds to the [Fe]-hydrogenase apoenzyme under the reconstitution conditions used for **3i**. To alleviate this unspecific binding, 0.5 mM of **4i** was mixed with equimolar apoenzyme in the reconstitution mixture. The reconstitution solution was incubated on ice for 1 hour and the unbound compound was then removed by ultrafiltration. The IR spectrum of the reconstituted [Fe]-hydrogense revealed two major CO peaks at 2013 and 1953 cm^{-1}, associated with weak shoulder peaks at 2025 and 1970 cm^{-1}, respectively (Fig. 5d). The positions of the two major peaks are similar to those of [Fe]-hydrogenase reconstituted with the FeGP cofactor and **3i** (Fig. 5a). The positions of the shoulder peaks are similar to those of unbound **4i** (Fig. 5c), indicating that a small amount of **4i** was unspecifically bound to the

protein. Addition of GMP to the reconstitution solution decreased the relative intensities of the CO bands at 2025 and 1970 cm^{-1}, suggesting a decrease in the unspecific binding of **4i**. The activity of the **4i**-reconstituted protein was less than 0.01 U/mg in both catalytic reactions, which is at the detection limit of the enzyme assay. This finding indicates that 2-hydroxy group is crucial for reconstitution of the active enzyme.

DFT computations. The electronic properties of model complexes containing the 2-OH and 2-OMe groups are similar according to their IR spectra.[12,13] DFT computations also indicate that the energy barriers for H_2 binding and cleavage are similar for complexes **1** and **2**, if heterolytic H_2 cleavage involving the thiolate ligand is considered (Supplementary Fig. 1). Thus, the dramatic difference in the activity of semisynthetic enzymes incorporating **3i** and **4i** points to a different mechanism. Unlike the methoxy group, the hydroxy group can be deprotonated to form a strong base. In [FeFe]-hydrogenase, the amine nitrogen in the azadithiolate bridge acts as an internal base for heterolytic H_2 cleavage.[30] It is possible that the OH group in the FeGP cofactor, as well as in **3i**, is deprotonated and functions similarly to the amine base in [FeFe]-hydrogenase. This possibility was previously suggested by theoretical studies.[23,40] To further explain experimental observations, we employed DFT computations to compare two mechanisms using complex **5** in which the tert-butyl thiolate group of **2** is replaced by a smaller methyl thiolate ligand, which is a better mimic of the natural cysteine ligand (Fig. 6). One mechanism involves thiolate as the proton acceptor, while the other mechanism involves the deprotonated OH group as the proton acceptor. Considerations of various mechanistic pathways are described in Supplementary Figs. 7 and 8 and Supplementary Tables 2-4. Because substrate binding triggers H_2 activation in [Fe]-hydrogenase, the mechanisms involving substrate binding as the first step are most relevant (Fig. 6).

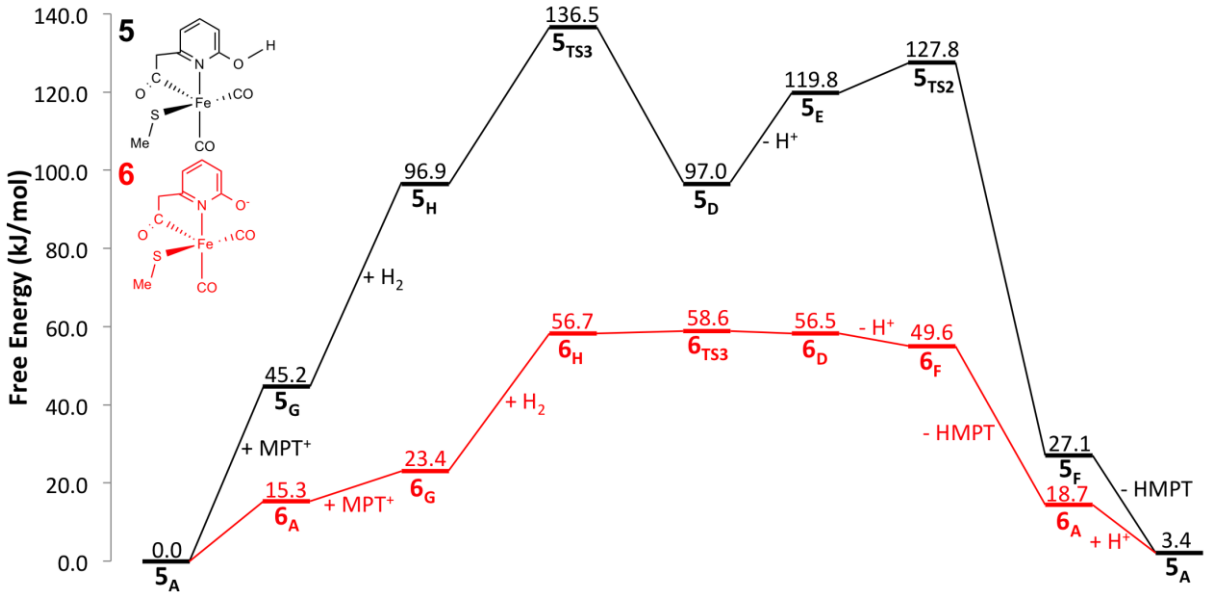

Figure 6 | Lowest energy reaction pathways for the catalytic cycles involving model complexes 5 and 6. Computations at the B3LYP-dDsC/TZ2P//M06/def2-SVP level in implicit THF solvent (COSMO-RS)]. MPT^+ is a truncated model of methenyl-H_4MPT^+ and was used as the hydride acceptor; 1-methylimiazole was used as the external proton acceptor. Compound numbering corresponds to the structures in Supplementary Fig. 7 and 8. The results indicate that the key steps in the catalysis are the deprotonation of 2-hydroxy group of the pyridinol ligand (5_A to 6_A) and the heterolytic H_2 activation using the 2-O^- group as an intramolecular proton acceptor.

For complex **5**, the lowest energy reaction pathway proceeds via MPT^+ association ($\mathbf{5_A} \rightarrow \mathbf{5_G}$), H_2 association ($\mathbf{5_G} \rightarrow \mathbf{5_H}$) and activation ($\mathbf{5_H} \rightarrow \mathbf{5_{TS3}} \rightarrow \mathbf{5_D}$), followed by proton removal utilizing 1-methylimidazole as an acceptor ($\mathbf{5_D} \rightarrow \mathbf{5_E}$). At this point a Fe-hydride species is formed, which can transfer the hydride to MPT^+ ($\mathbf{5_E} \rightarrow \mathbf{5_{TS2}} \rightarrow \mathbf{5_F}$) with a small barrier. The catalytic cycle is closed via the dissociation of HMPT to reform the starting catalyst ($\mathbf{5_F} \rightarrow \mathbf{5_A}$). The overall barrier of 137 kJ/mol is too high for the reaction to take place under biological conditions. On the other hand, deprotonation of the 2-OH group in **5** changes

the energy landscape dramatically. Deprotonation of **5** by 1-methylimidazole to form **6** is 15 kJ/mol uphill, and MPT^+ association ($\mathbf{6_A \rightarrow 6_G}$) now costs only 8 kJ/mol. The significantly lower energy cost for MPT^+ binding on **6** compared to **5** might be attributed to an electrostatic interaction of the electronegative 2-O^- group and the electropositive substrate, as suggested in a recent multi-scale modelling study.[40] H_2 binding costs an additional 33 kJ/mol ($\mathbf{6_G \rightarrow 6_H}$). Remarkably, heterolytic H_2 splitting utilizing the 2-O^- group as the internal base is extremely facile ($\mathbf{6_H \rightarrow 6_{TS3} \rightarrow 6_D}$), with a transition state barrier of only 2 kJ/mol. When $\mathbf{6_D}$ is deprotonated using 1-methylimidazole the hydride ligand spontaneously migrates to MPT^+ to form HMPT in an exergonic process ($\mathbf{6_D \rightarrow 6_F}$). Species analogous to 5_E and 5_{TS2} do not exist on the potential energy surface, consistent with the barrier-less hydride transfer. Finally, the original deprotonated catalyst can be reformed following dissociation of HMPT ($\mathbf{6_F \rightarrow 6_A}$). The highest point of the potential energy surface is 59 kJ/mol. Given the accuracy of DFT, this calculated energy barrier is in good agreement with the activity of the semisynthetic enzyme reconstituted from **3i**. Therefore, DFT computations clearly show that deprotonation of the 2-hydroxy group leads to an experimentally feasible catalytic cycle.

Cleavage of GMP. To test the effect of the GMP moiety on the function of the FeGP cofactor, the native cofactor was anoxically digested by phosphodiesterase I from *Crotalus adamanteus* venom at pH 8.9 in the presence of 1 mM 2-mercaptoethanol. Digestion of the FeGP cofactor was traced by UV-Vis measurements (Supplementary Fig. 9). The spectral change completed within 10 min in this assay, indicating that the FeGP cofactor was completely digested within 10 min under these reaction conditions. To verify the hydrolytic cleavage of the GMP moiety, the digested sample was decomposed with light and the masses of the decomposition products were determined by Matrix-assisted laser desorption/ionization mass spectrometry. In the mass spectrum, the peaks of the predicted decomposed product, 6-carboxymethyl-3,5-dimethyl-2-pyridone (*m/z* = 198), but not the non-digested

guanylylpyridinol [(6-carboxymethyl-3,5-dimethyl-4-hydroxy-2-pyridone-4-yl)-(5'-guanosyl) phosphate (*m/z* = 543)], were observed (Supplementary Fig. 10). This finding confirmed the cleavage of the phosphodiester linkage of the FeGP cofactor in the phosphodiesterase reaction. The [Fe]-hydrogenase reconstituted with this digested cofactor has a specific activity of 0.8 ± 0.2 U/mg for the reverse reaction. IR analysis showed that occupancy of the enzyme-digested cofactor in the protein was approximately 4% (Supplementary Fig. 11 and Supplementary Table 1). Assuming that the enzyme-digested cofactor is solely responsible for the activity (although the possibility of a trace amount of native FeGP cofactor in the enzyme is hard to rule out), the specific activity of the GMP-less native enzyme is 20 U/mg, which is a 10-fold decrease compared to the wild enzyme, but a 5-fold increase relative to the enzyme reconstituted with **3i**. This result is consistent with the significant roles of the GMP and the two methyl groups of the guanylylpyridinol ligand.

Discussion.

We successfully constructed an active [Fe]-hydrogenase from an apoenzyme and **3i**. This "semisynthetic" enzyme exhibited a higher turnover frequency than most known synthetic hydrogenation catalysts.[34,35] The iron centre in this reconstituted enzyme is most probably coordinated in the same manner as the iron ion in native [Fe]-hydrogenase, namely by one cysteine sulphur atom, two CO ligands, and the acyl carbon and pyridnyl nitrogen atoms of the 2-hydroxypyridinol ligand, as indicated by the IR spectrum (Fig. 5a). This ligand environment is nearly identical to that of complex **2**. Until now, all model complexes, including **1**-**4,** were inactive for H_2 activation despite having similar geometric and electronic structures to the active site of [Fe]-hydrogenase. The activity of this semisynthetic enzyme confirms the essential role of the protein environment for H_2 activation. The reconstituted [Fe]-hydrogenase with the 2-methoxy complex **4i** was inactive even with the complex being incorporated into the apoenzyme. This finding highlights the crucial role of the 2-hydroxy

group for the catalytic activity of [Fe]-hydrogenase. It is possible that the 2-hydroxy group serves to correctly position the cofactor in the protein. The crystal structure of [Fe]-hydrogenase shows that the Fe pyridinol complex is fixed onto the protein by a covalent bond through the cysteine-sulphur atom, a hydrogen bond through the acyl-oxygen atom, and multiple hydrophobic interactions through one of the CO ligands; the 2-hydroxy group appears to have no contact with protein (Supplementary Fig. 12) [4,8,10]. Therefore, the possibility of substantially different orientations of **3i** and **4i** in the reconstituted enzyme is unlikely. To account for the significantly different activity of the two semisynthetic enzymes, an alternative explanation is proposed, in which the hydroxy group is deprotonated and then functions as an internal base for heterolytic cleavage. DFT computations show this mechanism possesses a much lower activation barrier than the alternative mechanism in which the cysteine thiolate ligand serves as a proton acceptor. While some elements of the new mechanism were previously proposed,[23,40] the work described here provides the first experimental validation of this mechanism.

Substrate binding appears to be the trigger event for the function of [Fe]-hydrogenase. Without methenyl-H_4MPT$^+$, [Fe]-hydrogenase retains an open form and does not bind or activate H_2. Upon binding of methenyl-H_4MPT$^+$, [Fe]-hydrogenase adopts the closed form where H_2 binding and activation occur. Until now, it has been unclear how substrate binding and the resulting conformational change modify the reactivity of the active site. This study suggests that deprotonation of the 2-OH group is a key step for catalysis. Thus, we propose that [Fe]-hydrogenase controls its activity in the two conformations by allowing deprotonation only in the closed conformation. In the closed form, the 2-OH group could be located near the methenyl-H_4MPT$^+$ substrate in the active site pocket, which might change the pK value of this group[10] . Alternatively, as suggested by Reiher and co-workers in their DFT computations, the His14 group, which is located near the 2-hydroxy group, might play a role in modulating the pK of the 2-hydoxy moiety.[40]

The lower catalytic activity of the semisynthetic [Fe]-hydrogenase relative to the native enzyme may be due to the differences in 2-pyridinol ring substitution. The 3- and 5-methyl groups in the native cofactor will affect the electronic properties of the pyridinol nitrogen via their electron-donating effect. The 4-phosphate ester group will also affect the pK of the pyridinol nitrogen and could additionally contribute to cofactor binding[4]. The guanosine moiety of the 4-substituent contributes to the correct binding of the cofactor to the protein through an induced fit, consistent with the finding that in the presence of GMP the IR spectrum of the bound mimic sharpened (Fig. 5a) and the catalytic activity increased (Supplementary Fig. 5). The importance of the GMP moiety for the reconstitution of the active enzyme was also indicated by the enzymatic digestion study described above. Despite these differences, the activation energy for the semisynthetic [Fe]-hydrogenase reported here is only ~12 kJ/mol higher than the optimized native enzyme.

The reconstitution method developed here is general and can be applied to incorporate different synthetic mimics into the apoenzyme of [Fe]-hydrogenase. In the future, it may be possible to test, one by one, the contributions of the 3- and 5- methyl groups as well as of the 4-phosphoester group on the binding of iron-active-site and the subsequent activity. It may also be possible to test the contribution of the two CO ligands by synthesizing mimics with only one CO or with one CO and one cyanide in different configurations. The contribution of the sulphur ligand and of the second coordination sphere is accessible using mutated apoenzyme in the reconstitution experiments. These studies will hopefully contribute to our understanding of the necessary primary and secondary coordination environments for iron to activate H_2, a question of considerable applied interest.

Chemical modification strategies such as those described here are presently used to understand the structure and function relationship of the [FeFe] centre in [FeFe]-hydrogenases[30-32]. Learning how iron in [Fe]-hydrogenase functions may even contribute to our understanding of the role of iron in the [FeFe] centre of [FeFe]-hydrogenases and the

[NiFe] centre of [NiFe]-hydrogenases, in which the iron is also decorated with CO and other unusual ligands.

METHODS

Reconstitution of the [Fe]-hydrogenase holoenzyme. The model complex **3** (see Fig. 2 in the main text) was dissolved in methanol containing 1% acetic acid. For reconstitution of the [Fe]-hydrogenase holoenzyme, 0.4 ml of 10 mM **3i** solution was added anoxically into a 7.6 ml solution of 100 mM sodium acetate (pH 5.6), 0.02 mM apoenzyme, and 2 mM GMP (final concentrations) on ice and quickly and thoroughly mixed; the final concentrations of **3i** and the apoenzyme were 0.5 mM and 0.02 mM (25:1 ratio), respectively. Five % methanol contained in the reconstitution solution does not affect the stability of the apoenzymes. After incubation on ice for at least 1 hour, the reconstitution mixture was used for the catalytic activity assays. The reconstituted enzyme was unstable at room temperature and was completely inactivated after overnight incubation if not kept cool; activity of the enzyme reconstituted with the FeGP cofactor stays stable at room temperature in the same period. The instability of the enzyme reconstituted with the model complex could be attributed to the instability of the complex in relatively hydrophilic protein environment, probably because of the less hydrophilic character of the complex due to the absence of the GMP moiety. The enzyme reconstituted with **3i** was inactivated by light like the enzyme reconstituted with the FeGP cofactor. Therefore, the reconstituted enzyme solution was kept on ice during the experiments and used within several hours under dark conditions. For long-term storage, the reconstituted enzyme was shock-frozen in liquid nitrogen and stored at –75 °C. For IR spectroscopy, the reconstituted enzyme solution was concentrated to ~50 µl in a Millipore centrifuge concentrator with a 30-kDa cut-off ultra-filter. Then, the concentrated solution was

diluted more than ten-fold with anoxic water containing 2 mM GMP, and then concentrated again to 2–3 mM reconstituted enzyme with 2mM GMP. The sample without GMP was diluted with anoxic water in the absence of GMP and then concentrated. In the case of reconstitution in the absence of GMP, GMP was omitted throughout the experiments. For reconstitution with **4i**, 6.0 µl of 10 mM **4i** solution was added anoxically into a 0.25 ml solution containing 100 mM sodium acetate (pH 5.6), 0.5 mM apoenzyme, and 2 mM GMP (final concentrations) on ice and quickly and thoroughly mixed; the final concentrations of **4i** and the apoenzyme were 0.5 mM. After incubation on ice for at least 1 hour, the reconstitution mixture was used for the catalytic activity assays. For IR spectroscopy, the reconstituted enzyme solution was concentrated to ~20 µl in a Millipore centrifuge concentrator with a 30-kDa cut-off ultra-filter. Then, the concentrated solution was diluted more than ten-fold with anoxic water containing 2 mM GMP, and then concentrated again to 2–3 mM reconstituted enzyme with 2mM GMP. In the case of reconstitution in the absence of GMP, GMP was omitted throughout the experiments. Concentrated samples were stored in a Cryogenic Liquid Nitrogen Dry Shipper (Taylor-Wharton).

IR spectroscopy. All IR spectra were obtained with an FTIR spectrometer (Bruker, Vertex 70V) in an attenuated total reflection (ATR) optical configuration with Si prism of 45° incident angle and 2 active reflection (Smith Detection, DuraSamplIR IITM). Spectra were obtained with a resolution of 4 cm^{-1}. Five µl of the sample solutions were dropped on the effective area of a Si prism (3mm diameter) and concentrated by slowly evaporating solvent under mild flow of Ar gas. Hydration condition of the sample is estimated by relative intensities of water band (OH stretching mode) at around 3500 cm^{-1} against the amide II band of the protein at around 1550 cm^{-1}. Of the spectra that had been measured successively during the concentration process, we selected a spectrum of mildly hydrated sample that provided enough intensity to analyze the cofactor bands. A baseline correction had been made on the selected spectrum to eliminate contributions from the water overtone band around 2000 cm^{-1}.

Typically 512 spectra were co-added to obtain a sufficient signal-to-noise ratio. Measurement was handled under dark by covering the spectrometer with a blackout fabric in order to avoid light induced decomposition of the sample.

Computational Methods. Molecular structures were first optimized at the M06[41,42]/def2-SVP theoretical level using the SMD polarizable continuum model[43] for THF and the "Ultrafine" grid as implemented in Gaussian09.[44] Unscaled free energy correction was obtained from frequency computations on optimized geometries, which confirmed that all structures were either minima (zero imaginary frequencies) or transition states (one imaginary frequency) on the potential energy surface. Refined energy estimates, employing a density-dependent dispersion correction[45] appended to the B3LYP functional[46,47] (B3LYP-dDsC) to more accurately describe long-range dispersion interactions, were obtained via single point computations using the TZ2P slater-type orbital basis set in ADF.[48]

Acknowledgments We thank Prof. Dr. Rolf Thauer for discussions and helpful suggestions. Prof. Dr. Clémence Corminboeuf and LCMD at EPFL is acknowledged for providing computational resources. This work was supported by grants of the Max Planck Society (to R. Thauer) and of the PRESTO program from the Japan Science and Technology Agency to S. Shima, a grant of the National Natural Science Foundation of China (No. 21302028) to D. Chen, and grants from the Swiss National Science Foundation (200020_134473/1 and 200020_152850/1) to X. Hu. The authors declare no conflict of interests.

Author Contributions S.S. and X.H. directed the research. S.S., D.C. and X.H. designed the study. D.C., T.X, and K.M.S synthesized the model compounds. S.S. reconstituted and characterized the semisynthetic [Fe]-hydrogenase. J.K. performed MALDI-TOF-MS analysis.

K.A. performed IR spectroscopy with S.S. and T.F.. M.D.W. did the computations. S.S. and X.H. wrote the manuscript with contributions from all coauthors.

Author Information Reprints and permissions information is available at www.nature.com/reprints. The authors declare no competing financial interests. Readers are welcome to comment on the online version of the paper. Correspondence and requests for materials should be addressed to S.S. (shima@mpi-marburg.mpg.de) or X.H. (xile.hu@epfl.ch).

Reference

1 Vignais, P. M. & Billoud, B. Occurrence, classification, and biological function of hydrogenases: an overview. *Chem. Rev.* **107**, 4206-4272, (2007).
2 Fontecilla-Camps, J. C., Volbeda, A., Cavazza, C. & Nicolet, Y. Structure/function relationships of [NiFe]- and [FeFe]-hydrogenases. *Chem. Rev.* **107**, 4273-4303, (2007).
3 Lubitz, W., Ogata, H., Rudiger, O. & Reijerse, E. Hydrogenases. *Chem. Rev.* **114**, 4081-4148, (2014).
4 Shima, S. *et al.* The crystal structure of [Fe]-hydrogenase reveals the geometry of the active site. *Science* **321**, 572-575, (2008).
5 Shima, S. & Ermler, U. Structure and Function of [Fe]-Hydrogenase and its Iron-Guanylylpyridinol (FeGP) Cofactor. *Eur. J. Inorg. Chem.*, 963-972, (2011).
6 Buurman, G., Shima, S. & Thauer, R. K. The metal-free hydrogenase from methanogenic archaea: evidence for a bound cofactor. *FEBS Lett.* **485**, 200-204, (2000).
7 Shima, S. *et al.* The cofactor of the iron-sulfur cluster free hydrogenase Hmd: Structure of the light-inactivation product. *Angew. Chem., Int. Ed.* **43**, 2547-2551, (2004).
8 Hiromoto, T. *et al.* The crystal structure of C176A mutated [Fe]-hydrogenase suggests an acyl-iron ligation in the active site iron complex. *FEBS Lett.* **583**, 585-590, (2009).
9 Vogt, S., Lyon, E. J., Shima, S. & Thauer, R. K. The exchange activities of [Fe] hydrogenase (iron-sulfur-cluster-free hydrogenase) from methanogenic archaea in comparison with the exchange activities of [FeFe] and [NiFe] hydrogenases. *J. Biol. Inorg. Chem.* **13**, 97-106, (2008).
10 Hiromoto, T., Warkentin, E., Moll, J., Ermler, U. & Shima, S. The Crystal Structure of an [Fe]-Hydrogenase-Substrate Complex Reveals the Framework for H-2 Activation. *Angew. Chem., Int. Ed.* **48**, 6457-6460, (2009).
11 Chen, D., Scopelliti, R. & Hu, X. [Fe]-hydrogenase models featuring acylmethylpyridinyl ligands. *Angew. Chem. Int. Ed.* **49**, 7512-7515, (2010).
12 Chen, D., Scopelliti, R. & Hu, X. A five-coordinate iron center in the active site of [Fe]-hydrogenase: hints from a model study. *Angew. Chem. Int. Ed.* **50**, 5671-5673, (2011).
13 Hu, B., Chen, D. & Hu, X. Synthesis and reactivity of mononuclear iron models of [Fe]-hydrogenase that contain an acylmethylpyridinol ligand. *Chem. Eur. J.* **20**, 1677-1682, (2014).

14 Turrell, P. J., Wright, J. A., Peck, J. N. T., Oganesyan, V. S. & Pickett, C. J. The Third Hydrogenase: A Ferracyclic Carbamoyl with Close Structural Analogy to the Active Site of Hmd. *Angew. Chem., Int. Ed.* **49**, 7508-7511, (2010).
15 Schultz, K. M., Chen, D. & Hu, X. [Fe]-hydrogenase and models that contain iron-acyl ligation. *Chem. Asian. J.* **8**, 1068-1075, (2013).
16 Song, L. C. *et al.* Synthesis, structural characterization, and some properties of 2-acylmethyl-6-ester group-difunctionalized pyridine-containing iron complexes related to the active site of [Fe]-hydrogenase. *Dalton Trans.* **43**, 8062-8071, (2014).
17 Royer, A. M., Salomone-Stagni, M., Rauchfuss, T. B. & Meyer-Klaucke, W. Iron Acyl Thiolato Carbonyls: Structural Models for the Active Site of the [Fe]-Hydrogenase (Hmd). *J. Am. Chem. Soc.* **132**, 16997-17003, (2010).
18 Tard, C. & Pickett, C. J. Structural and functional analogues of the active sites of the [Fe]-, [NiFe]-, and [FeFe]-hydrogenases. *Chem. Rev.* **109**, 2245-2274, (2009).
19 Camara, J. M. & Rauchfuss, T. B. Combining acid-base, redox and substrate binding functionalities to give a complete model for the FeFe -hydrogenase. *Nat. Chem.* **4**, 26-30, (2012).
20 Ogo, S. *et al.* A Functional NiFe Hydrogenase Mimic That Catalyzes Electron and Hydride Transfer from H-2. *Science* **339**, 682-684, (2013).
21 Tao, X., Dafa, C. & Hu, X. Hydrogen-activating models of hydrogenases. *Coord. Chem. Rev.* **303**, 32-41, (2015).
22 Shima, S., Schick, M., Ataka, K., Steinbach, K. & Linne, U. Evidence for acyl–iron ligation in the active site of [Fe]-hydrogenase provided by mass spectrometry and infrared spectroscopy. *Dalton Trans.* **41**, 767-771, (2012).
23 Yang, X. Z. & Hall, M. B. Monoiron hydrogenase catalysis: Hydrogen activation with the formation of a dihydrogen, Fe-$H^{\delta-}$ --- H delta$^{\delta+}$-O, bond and methenyl-H_4MPT^+ triggered hydride transfer. *J. Am. Chem. Soc.* **131**, 10901-10908, (2009).
24 Finkelmann, A. R., Stiebritz, M. T. & Reiher, M. Kinetic Modeling of Hydrogen Conversion at Fe Hydrogenase Active-Site Models. *J. Phys. Chem. B* **117**, 4806-4817, (2013).
25 Dey, A. Density Functional Theory Calculations on the Mononuclear Non-Heme Iron Active Site of Hmd Hydrogenase: Role of the Internal Ligands in Tuning External Ligand Binding and Driving H-2 Heterolysis. *J. Am. Chem. Soc.* **132**, 13892-13901, (2010).
26 Wodrich, M. D. & Hu, X. Electronic elements governing the binding of small molecules to a Fe -hydrogenase mimic. *Eur. J. Inorg. Chem.* **2013**, 3993-3999, (2013).
27 Murray, K. A., Wodrich, M. D., Hu, X. L. & Corminboeuf, C. Toward functional type III [Fe]-hydrogenase biomimics for H2 activation: insights from computation *Chem.-Eur. J.* **21**, 3987-3996, (2015).
28 Ma, K., Zirngibl, C., Linder, D., Stetter, K. O. & Thauer, R. K. N^5, N^{10}-methylenetetrahydromethanopterin dehydrogenase (H_2-forming) from the extreme thermophile *Methanopyrus kandleri*. *Arch. Microbiol.* **156**, 43-48, (1991).
29 Zirngibl, C. *et al.* H_2-forming methylenetetrahydromethanopterin dehydrogenase, a novel type of hydrogenase without Iron-sulfur clusters in methanogenic archaea. *Eur. J. Biochem.* **208**, 511-520, (1992).
30 Berggren, G. *et al.* Biomimetic assembly and activation of FeFe -hydrogenases. *Nature* **499**, 66-69, (2013).
31 Esselborn, J. *et al.* Spontaneous activation of [FeFe]-hydrogenases by an inorganic [2Fe] active site mimic. *Nat Chem Biol* **9**, 607-609, (2013).
32 Siebel, J. F. *et al.* Hybrid FeFe -Hydrogenases with Modified Active Sites Show Remarkable Residual Enzymatic Activity. *Biochemistry* **54**, 1474-1483, (2015).

33 Shima, S., Schick, M. & Tamura, H. Preparation of [Fe]-hydrogenase from methanogenic archaea *Methods Enzymol* **494**, 119-137, (2011).
34 Bart, S. C., Lobkovsky, E. & Chirik, P. J. Preparation and molecular and electronic structures of iron(0) dinitrogen and silane complexes and their application to catalytic hydrogenation and hydrosilation. *J. Am. Chem. Soc.* **126**, 13794-13807, (2004).
35 Lagaditis, P. O. *et al.* Iron(II) Complexes Containing Unsymmetrical P-N-P ' Pincer Ligands for the Catalytic Asymmetric Hydrogenation of Ketones and Imines. *J. Am. Chem. Soc.* **136**, 1367-1380, (2014).
36 Shima, S. & Ataka, K. Isocyanides inhibit [Fe]-hydrogenase with very high affinity. *FEBS Lett.* **585**, 353-356, (2011).
37 Lyon, E. J. *et al.* Carbon monoxide as an intrinsic ligand to iron in the active site of the iron-sulfur-cluster-free hydrogenase H_2-forming methylenetetrahydromethanopterin dehydrogenase as revealed by infrared spectroscopy. *J . Am. Chem. Soc.* **126**, 14239-14248, (2004).
38 Korbas, M. *et al.* The iron-sulfur cluster-free hydrogenase (Hmd) is a metalloenzyme with a novel iron binding motif. *J. Biol. Chem.* **281**, 30804-30813, (2006).
39 Tamura, H. *et al.* Crystal structures of [Fe]-hydrogenase in complex with inhibitory isocyanides: implications for H_2-activation site *Angew. Chem. Int. Ed.* **52**, 9656-9659, (2013).
40 Finkelmann, A. R., Senn, H. M. & Reiher, M. Hydrogen-activation mechanism of [Fe] hydrogenase revealed by multi-scale modeling *Chem. Sci.* **5**, 4474-4482, (2014).
41 Zhao, Y. & Truhlar, D. G. The M06 suite of density functionals for main group thermochemistry, thermochemical kinetics, noncovalent interactions, excited states, and transition elements: two new functionals and systematic testing of four M06-class functionals and 12 other functionals. *Theor. Chem. Acc.* **120**, 215-241, (2008).
42 Zhao, Y. & Truhlar, D. G. Density functionals with broad applicability in chemistry. *Acc. Chem. Res.* **41**, 157-167, (2008).
43 Marenich, A. V., Cramer, C. J. & Truhlar, D. G. Universal Solvation Model Based on Solute Electron Density and on a Continuum Model of the Solvent Defined by the Bulk Dielectric Constant and Atomic Surface Tensions. *J. Phys. Chem. B* **113**, 6378-6396, (2009).
44 Gaussian 09, revision D.01 (Gaussian, Inc., Wallingford, CT, 2009).
45 Steinmann, S. N. & Corminboeuf, C. Comprehensive Bench marking of a Density-Dependent Dispersion Correction. *J. Chem. Theory Comp.* **7**, 3567-3577, (2011).
46 Becke, A. D. Density-Functional Thermochemistry. 3. The Role of Exact Exchange *J. Chem. Phys.* **98**, 5648-5652, (1993).
47 Lee, C. T., Yang, W. T. & Parr, R. G. Development of the Colle-Salvetti Correlation-Energy Formula into A Funcitonal of the Electron-Density *Phys. Rev. B* **37**, 785-789, (1988).
48 ADF2013 (SCM, Amsterdam).